ITALIAN SEISMIC RISK MAPS BASED ON CODE-COMPLIANT DESIGN

Chioccarelli Eugenio

Dipartimento di Ingegneria Civile, dell'Energia, dell'Ambiente e dei Materiali, Università degli Studi Mediterranea di Reggio Calabria, Italy. E-mail: eugenio.chioccarelli@unirc.it

Pacifico Adriana

Dipartimento di Strutture per l'Ingegneria e l'Architettura, Università degli Studi di Napoli Federico II, Italy. E-mail: adriana.pacifico@unina.it

Iervolino Iunio

Dipartimento di Strutture per l'Ingegneria e l'Architettura, Università degli Studi di Napoli Federico II, Italy. E-mail: iunio.iervolino@unina.it

This paper discusses the Italian seismic risk assuming that the existing buildings portfolio is substituted by new code-conforming structures. The seismic risk is quantified, at municipality scale, via the evaluation of failure rate per building class. This requires: (i) the probability that the structures fail for a given ground motion intensity value, that is, the fragility functions and (ii) the hazard curves resulting from probabilistic seismic hazard analyses. The adopted fragility functions come from the Italian research project RINTC – *Rischio Implicito delle Strutture progettate secondo le NTC*, in which a large set of buildings was designed for three sites representative of different seismicity. Thus, the Italian municipalities were divided in three seismic classes and it was assumed that fragility functions from RINTC are representative of new design (residential) structures, according to a replacement criterion that was established to associate the structural typologies of the existing buildings to those considered in the project. The failure rates per building typology were computed first, combining the structural fragility functions and the computed hazard curves. Then, the failure rates were averaged over the building typologies and the percentages of soil conditions characterizing each municipality. The results, presented in the form of maps, show that the fragility of masonry structures have the main impact on the maps, which are also affected by the identification of the hazard and soil classes of the sites.

Keywords: code-conforming structures, building classes, seismic failure rates, fragility functions, probabilistic seismic hazard analysis.

1. Introduction

Italy has enforced a building code (CS.LL.PP., 2008) that follows the modern principles of earthquake engineering, such as design actions based on probabilistic seismic hazard analysis, PSHA (McGuire, 1995), and performance-based design. Nevertheless, the Italian building stock is, for the vast majority, made of buildings built before the establishment of any formal seismic code, or with codes that can now be considered obsolete. This is one of the reasons why Italy is considered a high-risk country with respect to earthquakes. On the other hand, also the current code implicitly exposes structures to some implicit seismic risk (Iervolino et al., 2017). Therefore, it is worthwhile to investigate what the risk in the country would be if the building stock were of new design. This is the subject of the study herein presented; here a hypothetical scenario in which all the existing residential buildings are replaced by new code-conforming structures is considered. The vulnerability of the new design structures is modelled in accordance with an Italian research program, named *Rischio Implicito delle Strutture progettate secondo le NTC* or RINTC (RINTC-Workgroup 2018), that designed and analysed a large set of code-conforming buildings located in some Italian sites, representative of different seismic hazard levels.

In this work, the seismic risk is quantified, at the municipality scale, in terms of annual failure rate, that is the mean number of earthquakes that in one year cause structural failure of a (randomly selected) building of the municipality of interest. Such a rate is a function of the seismic hazard, the seismic vulnerability of the structural typologies and the proportion among different structural typologies in the municipality. The failure rate is defined with respect to two different performance levels: (i) usability-preventing damage, representative of non-structural elements damage and (ii) global collapse, intended as life-safety-threatening structural failure. The failure rates are, first, defined for each structural typology combining the structural fragility and the result of a probabilistic seismic hazard analysis (i.e., the hazard curve) and considering the local soil conditions. Then, a failure rate per municipality is computed in accordance with the percentage of each structural typology within the municipality. The maps of resulting failure rates are used to quantify the seismic risk.

Proceedings of the 31st European Safety and Reliability Conference
Edited by Bruno Castanier, Marko Cepin, David Bigaud, and Christophe Berenguer
Published by Research Publishing, Singapore.
ISBN: 978-981-18-2016-8; doi:10.3850/978-981-18-2016-8_678-cd

The paper is structured such that the considered buildings among those of the RINTC project are presented first. Then, the methodology for risk assessment is described, identifying the hypotheses, the models and the quantitative information that are required for the analyses. Then, the probabilistic seismic hazard analyses, the characteristics of the existing building stock together with the replacement criteria and the identification of the local soil conditions are discussed. Thus, the maps of the seismic risk for Italian code-conforming structures are presented. A discussion and some final remarks close the paper.

2. Code conforming structures

In the RINTC project, a large set of both residential and industrial buildings was designed, in accordance with the current Italian building code (CS.LL.PP. 2018; 2008), to be ideally located in a few Italian sites chosen as representative of different levels of seismicity: L'Aquila, (AQ), Naples, (NA), and Milan, (MI), representative of high, medium, and low seismic hazard in the country, respectively. The considered structural typologies (*st*), identified by the construction material and the number of floors, are here listed and briefly described.

- Unreinforced masonry structures (URM) (Manzini et al., 2018; Cattari et al., 2018) – residential two- and three-story buildings made of perforated clay units with mortar joints varying among different architectural configurations and wall thickness (each architectural configuration is identified with the letter C or E and a number). All the considered structures are regular buildings, according to the definition provided by the Italian code.
- Reinforced concrete (RC) buildings (Ricci et al., 2018) – three- and six-story, infilled (IF), moment resisting frame buildings, regular in plan and elevation. A single architectural configuration is considered.

Multiple-stripes nonlinear dynamic analysis, (MSA) (Jalayer and Cornell, 2009) were performed for three-dimensional models of the structures and the results were analysed with respect to two damage states (DSs): usability-preventing damage (UPD) and global collapse (GC). The onset of UPD is based on a multi-criteria approach; if one of following conditions occurs the structure is considered failed: (i) light damage in 50% of the main non-structural elements (e.g., infills); (ii) at least one of the non-structural elements reaches a severe damage level; (iii) first attainment of 95% of the maximum base-shear of the structure. The GC criterion is based on the deformation capacity (the roof displacement or the inter-story drift ratio) corresponding to 50% strength decay from the nonlinear static capacity curves of the structural model. Damage states are consistently defined for each structural typology (although their identification requires some additional details that depend on the considered typology, see Iervolino et al., 2018). The ground motion intensity measure (*IM*) adopted for the MSA is the spectral acceleration, *Sa*, at a period, *T*, close to the first vibration period of each model.

As pertaining to URM structures, the two-floor building in L'Aquila is modelled via five alternative architectural configurations whereas, in the same site, three configurations for the three-floor building are considered. In Naples, two and four configurations are considered for the two-story and three-story building, respectively. Finally, in Milan, three and four configurations are associated to the two-story and three-story building, respectively. For the *k-th* architectural configuration of each structural typology, the conditional failure probability given a IM value, $P\left[DS^{(st,k)} \geq ds|im\right]$, that is the building fragility function, was computed adopting a lognormal model:

$$P\left[DS^{(st,k)} \geq ds|im\right] = \Phi\left[\frac{ln(im)-\mu^{(st,k)}}{\sigma^{(st,k)}}\right], \quad (1)$$

where $\left\{\mu^{(st,k)}, \sigma^{(st,k)}\right\}$ are parameters.

Thus, in the following, the fragility for each structural typology at a specific site, $P\left[DS^{(st)} \geq ds|im\right]$, is computed combining $P\left[DS^{(st,k)} \geq ds|im\right]$ of the corresponding architectural configurations, as per Eq. (2):

$$P\left[DS^{(st)} \geq ds|im\right] = \sum_k P\left[DS^{(st,k)} \geq ds|im\right] \cdot w_{st,k}, \quad (2)$$

where $w_{st,k}$ weighs the representativeness of the architectural configuration in the actual building portfolio (assuming that these configurations completely cover the building stock). As anticipated, for RC structures, one architectural configuration is considered at each site; thus, in Eq. (1) and Eq.(2), k and w_k are both equal to one. Table 1 summarizes the fragility parameters (assuming the IM in g) for all the configurations for both performance levels at the three sites considered by the RINTC project; such a parameters were computed from the outputs of the MSA via the R2R-software (Baraschino et al., 2020).

Table 1 – Analysed structures: site of design, intensity measure, number of floors, architectural configuration, structural typology, fragility functions parameters, and weights.

Site	IM	Storey	Configuration	Typology	UPD μ	UPD σ	GC μ	GC σ	w_k
AQ	$Sa(0.15s)$	3	IF	RC	-0.438	0.414	1.791	0.661	1
AQ	$Sa(0.5s)$	6	IF	RC	-0.330	0.388	1.329	0.235	1

Table 1 – (Continued)

NA	$Sa(0.15s)$	3	IF	RC	-0.076	0.512	1.498	0.670	1
NA	$Sa(0.5s)$	6	IF	RC	-1.108	0.494	1.411	0.322	1
MI	$Sa(0.15s)$	3	IF	RC	0.060	0.515	0.303	0.318	1
MI	$Sa(0.5s)$	6	IF	RC	-0.547	0.290	0.400	0.309	1
AQ	$Sa(0.15s)$	2	E2	URM	-0.0416	0.197	0.6018	0.342	0.2
AQ	$Sa(0.15s)$	2	E5	URM	-0.324	0.26	0.5569	0.427	0.2
AQ	$Sa(0.15s)$	2	E8	URM	-0.2477	0.189	0.6114	0.321	0.2
AQ	$Sa(0.15s)$	2	E9	URM	-0.1126	0.177	0.2793	0.262	0.2
AQ	$Sa(0.15s)$	2	C3	URM	-0.6597	0.313	0.5153	0.282	0.2
AQ	$Sa(0.15s)$	3	E2	URM	-0.2472	0.400	0.4239	0.535	0.33
AQ	$Sa(0.15s)$	3	E8	URM	-0.2634	0.362	0.4680	0.514	0.33
AQ	$Sa(0.15s)$	3	C1	URM	-1.0477	0.222	0.2356	0.456	0.33
NA	$Sa(0.15s)$	2	C1	URM	-0.7190	0.245	0.9457	0.421	0.44
NA	$Sa(0.15s)$	2	C4	URM	-0.5712	0.307	0.9549	0.349	0.56
NA	$Sa(0.15s)$	3	E2	URM	-0.0775	0.540	0.8766	0.245	0.27
NA	$Sa(0.15s)$	3	E8	URM	-0.1181	0.490	0.8649	0.323	0.27
NA	$Sa(0.15s)$	3	C3	URM	-0.8726	0.277	0.7328	0.340	0.27
NA	$Sa(0.15s)$	3	C5	URM	-0.8562	0.245	0.7294	0.417	0.2
MI	$Sa(0.15s)$	2	E2	URM	0.1408	0.164	0.2961	0.124	0.41
MI	$Sa(0.15s)$	2	C1	URM	-0.3638	0.339	0.2234	0.150	0.18
MI	$Sa(0.15s)$	2	C7	URM	-0.6589	0.202	0.5061	0.112	0.41
MI	$Sa(0.15s)$	3	E2	URM	-0.1728	0.262	-0.4146	0.081	0.27
MI	$Sa(0.15s)$	3	E8	URM	-0.5548	0.174	-0.3894	0.131	0.27
MI	$Sa(0.15s)$	3	E9	URM	-0.7550	0.101	-0.6340	0.094	0.27
MI	$Sa(0.15s)$	3	C2	URM	-0.8495	0.311	0.6157	0.194	0.18

3. Methodology

Considering a site, in which there is exposure to seismic risk, affected by a number of seismic sources (s), the rate of earthquakes causing the exceedance of an IM threshold for a specific (known) soil class, that is $\lambda_{im|\theta}$, is provided by Eq.(3):

$$\lambda_{im|\theta} = \sum_{s} \nu_s \cdot \int_r \int_m P[IM > im | M_s = m, R_s = r, \theta] \cdot \cdot f_{M_s,R_s}(m,r) \cdot dm \cdot dr. \quad (3)$$

In the equation, the subscript s identifies the seismic source, M_s is the magnitude and R_s is the source-to-site distance, ν_s is the annual rate of earthquakes with magnitude higher than a threshold occurring on the source, $f_{M_s,R_s}(m,r)$ is the joint probability density function (PDF) of M_s and R_s, and $P[IM > im | M_s = m, R_s = r, \theta]$ is the probability that an earthquake of magnitude $M_s = m$ and distance $R_s = r$ causes the exceedance of the im at the site, usually provided by a ground motion prediction equation (GMPE) and depends, at least, on the soil condition at the site of interest that is represented by the θ parameter. The plot of $\lambda_{im|\theta}$ versus the possible im values is the so-called hazard curve (McGuire, 1995).

Considering one building of a given structural typology and located on a known soil class, the rate of earthquakes causing the building to fail, that is, to reach or exceed a damage state ($DS \geq ds$), $\lambda_{DS^{(st)} \geq ds|\theta}$, can be computed via Eq. (4) in which it is assumed that the fragility of the structural typology is not dependent on the soil condition of the construction site and $|d\lambda_{im|\theta}(z)|$ is the absolute value of the derivative of the hazard curve at $IM = z$:

$$\lambda_{DS^{(st)}\geq ds|\theta} = \int_{im} P\left[DS^{(st)} \geq ds|z\right] \cdot \left|d\lambda_{im|\theta}(z)\right|. \quad (4)$$

When the site is representative of an entire municipality (e.g., the centroid of its area), the soil condition at the base of each building is usually unknown. However, it may be possible to compute the probability that a generic building of the considered structural typology is located on each possible soil condition, $P[\theta_i]$. Applying the total probability theorem, Eq. (5) replaces Eq. (4):

$$\lambda_{DS^{(st)}\geq ds} = \sum_i \left\{\int_{im} P\left[DS^{(st)} \geq ds|z\right] \cdot \left|d\lambda_{im|\theta_i}(z)\right|\right\} \cdot P[\theta_i]. \quad (5)$$

If the probability that a building of the municipality belongs to a given structural typology, $P[st]$, can be computed, the rate of earthquakes causing the *typical* building to reach or exceed a damage state, λ_{ds}, can be computed via Eq. (6), where it is assumed that soil condition and structural typology are independent RVs:

$$\lambda_{ds} = \sum_{st} \lambda_{DS^{(st)}\geq ds} \cdot P[st] =$$
$$= \sum_{st} \sum_i \left\{\int_{im} P\left[DS^{(st)} \geq ds|z\right] \cdot \left|d\lambda_{im|\theta_i}(z)\right|\right\} \cdot P[\theta_i] \cdot P[st]. \quad (6)$$

In accordance with the classical hypothesis of the PSHA and the performance-based earthquake engineering (Cornell and Krawinkler, 2000), the process of earthquake occurrence causing the generic structure to fail is a homogenous Poisson process. Thus, λ_{ds} allows computing the expected number of failed buildings in the municipality in a time interval $(t, t+\Delta t)$; if Δt is small, it can be approximated by Eq. (7):

$$E\left[N_{ds,(t,t+\Delta t)}\right] \approx N_B \cdot \lambda_{ds} \cdot \Delta t, \quad (7)$$

in which N_B is the total number of buildings of the municipality. (Note that the computed rate, practically, has not any other meaning that its use in this last equation, that is to compute the expected value of damaged buildings).

4. Input data for nationwide code-conforming risk assessment

The following sections discusses the way the terms involved in the previous equations are defined in order to compute λ_{ds} for each Italian municipality and assuming a hypothetical scenario in which all the structures are new code-conforming buildings.

4.1. Seismic hazard

The official (i.e., adopted by the Italian building code, CS.LL.PP. 2008; 2018) assessment of the Italian seismic hazard considers the earthquakes can be generated in thirty-six seismogenic zones as described in Meletti et al. (2008) (see Fig. 1b) and adopts a logic-tree constituted by sixteen branches (Stucchi et al. 2011). The branch named 921, claimed to produce the closest results to those of the whole logic-tree, is the one adopted herein for PSHA. More specifically, the implemented ground motion prediction equation is Ambraseys et al. (1996) and the magnitude distribution of each seismic zone is described via the so-called *activity rates* (Iervolino et al., 2018).[a] The considered *IM*s are the pseudo-spectral acceleration at the vibration periods of interest of the structures (see Table 1) and the peak ground acceleration, PGA, (see Section 4.2).

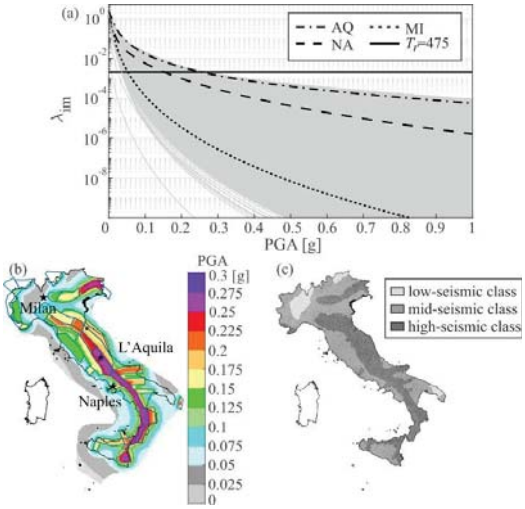

Fig. 1 – Hazard curves for PGA on rock for all Italian municipalities, (except Sardinia) (a), map of PGA_{475} together with the seismogenic zones of Meletti et al. (2008) (b), and seismic class for each Italian municipality (see Section 4.2) (c).

For each municipality, PSHA was performed (at the site identified as the centroid of the municipality area), Eq. (3), considering about eight thousand values of the selected intensity measures ranging from 0 to 20g. All the analyses are performed via the REASSESS software (Chioccarelli et al. 2019). Fig. 1a shows the hazard curves for PGA on rock soil conditions computed for the all the municipalities.[b] In the same figure, the hazard curves for Milan, Naples and L'Aquila are identified together with the exceedance rate corresponding to a return period (T_r) of 475 years, that is a reference value for design of new structures and will be adopted in the following for the identification of seismic classes (see Section 4.2). The values of PGA corresponding to $T_r = 475$, that is PGA_{475}, are reported in Fig. 1b.

4.2. Seismic classes and replacement criteria

RINTC results are incomplete for the purposes of this project, in the sense that the studied sites and structural typologies cannot be directly representative of the whole Italian territory and building stock. Thus, some criteria to replace the existing buildings with the code-conforming structures from RINTC were adopted. For each municipality, the number of existing residential RC and

[a] These choices are in accordance with the hazard evaluation involved in the record selections used for nonlinear dynamic analyses in RINTC project.

[b] Sardinia is not considered hereafter for seismic reliability assessment because, according to the cited source model, it is outside the definition range of the GMPE.

masonry buildings of one, two, three, and more than three stories was retrieved from IRMA (Borzi et al., 2020). Then, the following criteria were adopted: the RC buildings with three stories, or less, were replaced by new three-story RC buildings (RC_3), whereas RC buildings with more than three stories are substituted by new six-story buildings (RC_6); the masonry buildings with one or two stories are substituted by new two-story URM (URM_2), and the three-story masonry buildings are substituted by new three-story URM (URM_3). Finally, masonry buildings with more than three stories are replaced with RC_6 assuming that new design masonry buildings with more than three story are unusual.

The probability that a building belongs to one of the considered structural typology, $P[st]$ from Eq. (6), where st corresponds, in turn, to RC_3, RC_6, URM_2, URM_3, is computed as the number of buildings of that structural typology divided by the total number of buildings in the considered municipality (after the replacement). Fig. 2 shows, for each municipality, the computed probability; in most of the municipalities, the prevalent structural typology is URM_2, whereas URM_3 and RC_3 are present on the whole territory and RC_6 are concentrated in a few sites (i.e., the major Italian cities).

Since the available fragility functions refer to structures designed in AQ, NA and MI, the Italian municipalities were divided in three seismic classes based on their PGA_{475} on rock soil conditions (see Fig. 1b). The thresholds of the classes are the PGA_{475} values of Milan and Naples, so that municipalities with PGA_{475} lower than Milan are in the low seismic class; municipalities with PGA_{475} higher than Naples are in the high seismic class; all the remaining municipalities are in the medium seismic class.

The resulting classification is represented in Fig. 1c: 15% of the Italian municipalities are in the low seismic class, 48% correspond to medium seismicity and 37% to high seismicity. Thus, fragility functions of the structures designed in Milan, Naples and L'Aquila are considered as representative of the new-designed structures in municipalities of low, medium and high seismicity class, respectively. Even if this choice causes some approximations, it was preferred with respect to the artificial modification of fragility parameters to match the seismicity level of different sites.[c]

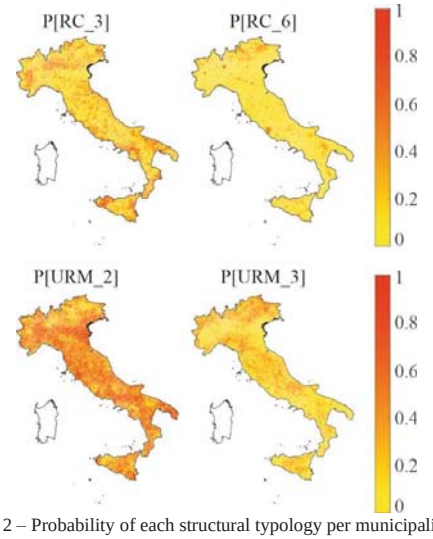

Fig. 2 – Probability of each structural typology per municipality.

4.3. Local soil conditions

According to Eq. (5) and Eq. (6), the probability that the building of a given municipality is located on a specific soil class, is required. It is computed profiting of the work of Forte et al. (2019) that provided, for the whole Italy, the soil classes according to (CEN 2003), indicated with letters from A to D. The latter are converted, for the purposes of this study, into the classes of the considered GMPEs (Section 4.1); i.e., rock, stiff and soft soil. In particular, A corresponds to rock, whereas B corresponds to stiff soil and C-D correspond to soft soil.

The grid of soil classes from Forte et al. (2019) was superimposed to the map of the urbanized areas provided by the *Italian Istituto Nazionale di Statistica* (ISTAT) and, in each municipality, the soil class probability, $P[\theta_i]$ with $\theta_i = \{rock, stiff, soft\}$, is computed as the number of grid points of a given soil class divided by the total grid points within the urbanized areas. The resulting probabilities are reported in Fig. 3. As shown, the highest probability is associated to stiff soil in most of the municipalities; soft soil covers a non-negligible number of urbanized areas and is predominant in the north-eastern municipalities and along the coasts; finally, rock soil is significant only in few areas (in Puglia and Sicily).

[c] Similar to the case of building substitution, such a classification is arbitrary although it was verified that alternative criteria, not shown here for the sake of brevity, do not provide preferable results (see the also Section 5).

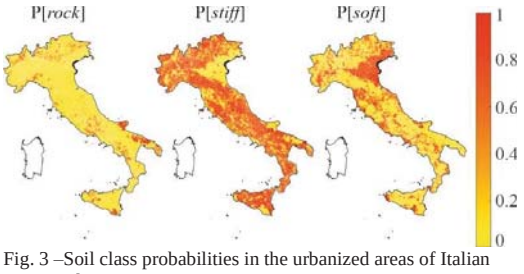

Fig. 3 –Soil class probabilities in the urbanized areas of Italian municipalities.

5. Results

The failure rate for each municipality are computed according to Eq. (6) referring to the two damage states described in Section 2. The resulting maps are reported in Fig. 4. In both the cases, computed values lower than 1E-5 are substituted by 1E-5 because low failure rates depend on hazard and fragility models extrapolated to be representative of large ground motion intensity values. Thus, to avoid that results were affected by significant hazard extrapolations, 1E-5 was (arbitrarily) identified as minimum threshold value.

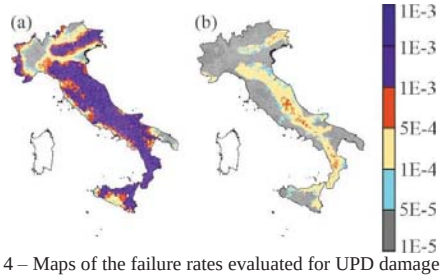

Fig. 4 – Maps of the failure rates evaluated for UPD damage state (a) and GC damage state (b).

As pertaining to the UPD, Fig. 4a, failure rates vary between 1E-5 to 6.68E-3 and most of the sites (46% of the municipalities) are characterized by rates larger than 1E-03; 32% of sites have rates within 1E-4 and 1E-3; about the 22% of municipalities have rate lower than 1E-4. Comparing Fig. 4a and Fig. 1c, the influence of the seismic class can be easily deduced. Indeed, in the low-seismic class, all the failure rates are lower than 5E-5, and 95% of the municipalities in the high-seismic class have rates higher than 1E-3.

Referring to the GC damage state, Fig. 4b, computed rates range from 1E-5 to 8.68E-4. Most of the sites (65%) presents a failure rate lower than 5E-5 and values higher than 5E-5 are observed only in the high-seismic class.[d]

As previously discussed, soil conditions are considered in PSHA and stiff soil (according to the selected GMPEs) is the most relevant over the country. Thus, it is expected that the rates associated to stiff soils are the closest to the shown results. To deepen this issue, the map of GC rates is computed assuming that all the sites have rock, stiff or soft soil conditions as shown in Fig. 5a, Fig. 5b and Fig. 5c, respectively. The graphical comparison of the figures confirms that the case of stiff soil provides the most similar distribution of failure rates to Fig. 4b.

However, to provide a synthetic, quantitative comparison of the maps, for each municipality, the ratio of the GC failure rates in Fig. 5 and those in Fig. 4b is computed and the average value over the country is reported. The average ratio computed referring to Fig. 5a, Fig. 5b and Fig. 5c is 0.79, 1.18 and 0.97, respectively. Thus, the case of soft soil provides closest results, in average, to those obtained considering the probability of each soil class.

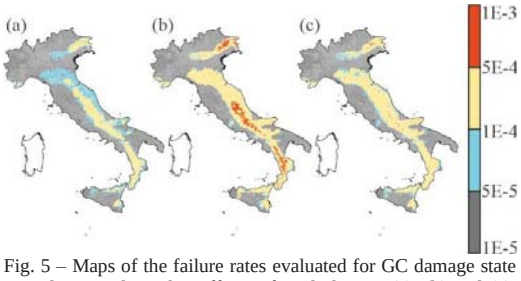

Fig. 5 – Maps of the failure rates evaluated for GC damage state considering only rock, stiff or soft soil class in (a), (b) and (c), respectively.

In Fig. 6 the influence of the structural typologies is shown by risk maps in which only one structural typology is adopted. Results show that for URM buildings (Fig. 6c and Fig. 6d) the computed failure rates are larger than those computed for RC buildings (Fig. 6a and Fig. 6b).

This is in accordance with one of the main results of the RINTC project: although the seismic actions at the base of the code are defined for the same exceedance probability independently on the construction' site and on the structural typology, the failure rate varies among the structures and the considered sites. To discuss which structural typology contributes the most to the aggregated results in Fig. 4b, the average ratio of the rates in Fig. 6 and those in Fig. 4b is computed: 0.63 is the average ration for RC_3, 0.67 for RC_6, 1.07 for URM_2, and 1.85 for URM_3. Thus, while RC buildings are less vulnerable than the average, URM two-story buildings provide results that are in average, over the country, close to the those of Fig. 4b. This is in accordance with Section 4.2 being such a structural typology the most probable in the Italian building portfolio after substitution of the existing buildings.

6. Conclusions

This work discusses the ideal seismic risk maps for Italy, i.e., the seismic structural reliability over the country assuming that all the buildings are replaced with code-

[d] The reported percentages refer to the number of municipalities and do not account for the geographical extension of each municipality.

conforming structures. For each municipality, the risk is quantified via the mean number of earthquakes, that in one year, cause the exceedance of a damage state (i.e., failure) of a generic building. Considered damaged states (performances identifying structural failure) are usability-preventing damage (UPD) and global collapse (GC). Replacement structures are selected among those studied in the RINTC project.

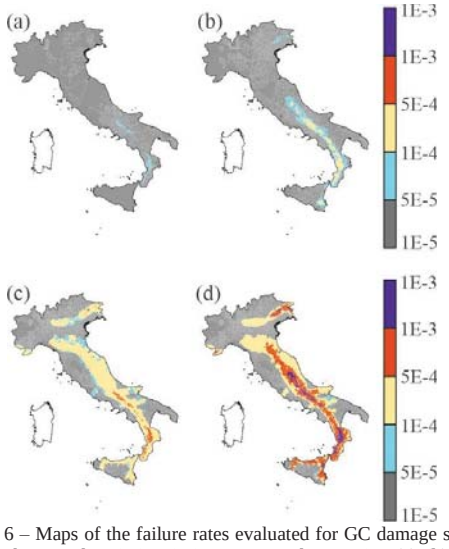

Fig. 6 – Maps of the failure rates evaluated for GC damage state considering only RC_3, RC_6, URM_2 and URM_3 in (a), (b), (c) and (d), respectively.

The results are in accordance with those observed for few sites in the RINTC project. Although the design actions are characterized by the same exceedance probability, the failure rates are different among different structural typologies and sites. UPD failure rates, over the country, vary between 1E-5 and 6.68E-3; 45% of the municipalities are characterized by failure rates larger than 1E-3 while all the others are lower. Referring to the GC, failure rates range from 1E-5 to 8.68E-4 and the most of Italian municipalities (65%) shows a failure rate lower than 5E-5. The replacement criterion was proven to be significant for such results; indeed, failure rates have low variability within each identified seismic class. Moreover, due to the distribution of soil classes and composition of the existing building stock in Italy, it was shown that, assuming one single soil class (i.e., soft soil) or one single structural typology (i.e., two-story unreinforced masonry), provides a good approximation of the average failure rate in Italy.

Acknowledgement

The study was developed in the framework the ReLUIS-DPC 2014–2018 project, funded by the Italian Civil Protection Department.

References

Ambraseys, NN, KA Simpson, and JJ Bommer. (1996). Prediction of Horizontal Response Spectra in Europe. *Earthq. Eng. Struct. Dyn.* 25 (4): 371–400.

Baraschino, R, G Baltzopoulos, and I Iervolino. (2020). R2R-EU: Software for Fragility Fitting and Evaluation of Estimation Uncertainty in Seismic Risk Analysis. *Soil Dyn. Earthq. Eng.* 132 (2).

Borzi, B, M Onida, M Faravelli, D Polli, M Pagano, D Quaroni, A Cantoni, E Speranza, and C Moroni. (2020). IRMA Platform for the Calculation of Damages and Risks of Italian Residential Buildings. *Bull. Earthq. Eng.*

Cattari, S, D Camilletti, S Lagomarsino, S Bracchi, M Rota, and A Penna. (2018). Masonry Italian Code-Conforming Buildings. Part 2 : Nonlinear Modelling and Time-History Analysis. *J. Earthq. Eng.* 22 (2): 74–104.

CEN, (2003). TC250/SC8/ Eurocode 8: Design Provisions for Earthquake Resistance of Structures, Part 1.1: General Rules, Seismic Actions and Rules for Buildings.

Chioccarelli, E, P Cito, I Iervolino, and M Giorgio. (2019). REASSESS V2.0: Software for Single- and Multi-site Probabilistic Seismic Hazard Analysis. *Bull. Earthq. Eng.* 17 (4): 1769–93.

Cornell, CA, and H Krawinkler. (2000). Progress and Challenges in Seismic Performance Assessment. *PEER Cent. News* 3 (2).

CS.LL.PP. (2008). Norme Tecniche per Le Costruzioni. *Gazz. Uff. Della Repubb. Ital.* 29.

CS.LL.PP. (2018). Aggiornamento Delle Norme Tecniche per Le Costruzioni. *Gazz. Uff. Della Repubb. Ital.* 42: 1–198.

Forte, G, E Chioccarelli, M De Falco, P Cito, A Santo, and I Iervolino. (2019). Seismic Soil Classification of Italy Based on Surface Geology and Shear-Wave Velocity Measurements. *Soil Dyn. Earthq. Eng.* 122 (3): 79–93.

Iervolino, I, E Chioccarelli, and M Giorgio. (2018). Aftershocks' Effect on Structural Design Actions in Italy. *Bull. Seismol. Soc. Am.* 108 (4): 2209–20. doi.org/10.1785/0120170339.

Iervolino, I, A Spillatura, and P Bazzurro. (2017). RINTC Project - Assessing the (Implicit) Seismic Risk of Code-Conforming Structures in Italy. *Proc. 6th Int. Conf. Comput. Methods Struct. Dyn. Earthq. Eng. (COMPDYN 2015)*, June: 1545–57.

Iervolino, I, A Spillatura, and P Bazzurro. (2018). Seismic Reliability of Code-Conforming Italian Buildings. *J. Earthq. Eng.* 22 (2): 5–27.

Jalayer, F, and CA Cornell. (2009). Measuring Bias in Structural Response Caused by Ground Motion Scaling. *Earthq. Eng. Struct. Dyn.* 38: 951–72. https://doi.org/10.1002/eqe.876.

Manzini, CF, G Magenes, A Penna, F Porto, D Camilletti, S Cattari, and S Lagomarsino. (2018). Masonry Italian Code-Conforming Buildings. Part 1 : Case Studies and Design Methods. *J. Earthq. Eng.* 22 (2): 54–73.

McGuire, RK. (1995). Probabilistic Seismic Hazard Analysis and Design Earthquakes: Closing the Loop. *Bull. Seismol. Soc. Am.* 85 (5): 1275–84. doi.org/10.1016/0148-9062(96)83355-9.

Meletti, C, F Galadini, G Valensise, M Stucchi, R Basili, S Barba, G Vannucci, and E Boschi. (2008). A Seismic Source Zone Model for the Seismic Hazard Assessment of the Italian Territory. *Tectonophysics* 450: 85–108.

Ricci, P, V Manfredi, F Noto, M Terrenzi, C Petrone, F Celano, MT De Risi, et al. (2018). Modeling and Seismic Response Analysis of Italian Code-Conforming Reinforced Concrete Buildings. *J. Earthq. Eng.* 22 (2): 105–39.

RINTC-Workgroup. (2018). Results of the 2015-2018.The Iplicit Risk of Code-Conforming Structures in Italy (RINTC) Project. *ReLUIS Report, Rete Dei Lab. Univ. Di Ing. Sismica (ReLUIS), Naples, Italy*.

Stucchi, M, C Meletti, V Montaldo, H Crowley, GM Calvi, and E Boschi. (2011). Seismic Hazard Assessment (2003-2009) for the Italian Building Code. *Bull. Seismol. Soc. Am.* 101 (4): 1885–1911.